Cell Stress and Chaperones (2020) 25:1045–1058
https://doi.org/10.1007/s12192-020-01141-w

ORIGINAL PAPER

BAG3 and BAG6 differentially affect the dynamics of stress granules by targeting distinct subsets of defective polypeptides released from ribosomes

Laura Mediani[1] · Veronica Galli[1] · Arianna Dorotea Carrà[1] · Ilaria Bigi[1] · Jonathan Vinet[1] · Massimo Ganassi[1] · Francesco Antoniani[1] · Tatiana Tiago[1] · Marco Cimino[1] · Daniel Mateju[2] · Cristina Cereda[3] · Orietta Pansarasa[3] · Simon Alberti[2,4] · Jessica Mandrioli[5] · Serena Carra[1]

Received: 26 May 2020 / Revised: 10 July 2020 / Accepted: 15 July 2020 / Published online: 21 July 2020

Abstract

Stress granules (SGs) are dynamic ribonucleoprotein granules induced by environmental stresses. They play an important role in the stress response by integrating mRNA stability, translation, and signaling pathways. Recent work has connected SG dysfunction to neurodegenerative diseases. In these diseases, SG dynamics are impaired because of mutations in SG proteins or protein quality control factors. Impaired SG dynamics and delayed SG dissolution have also been observed for SGs that accumulate misfolding-prone defective ribosomal products (DRiPs). DRiP accumulation inside SGs is controlled by a surveillance system referred to as granulostasis and encompasses the molecular chaperones VCP and the HSPB8-BAG3-HSP70 complex. BAG3 is a member of the BAG family of proteins, which includes five additional members. One of these proteins, BAG6, is functionally related to BAG3 and able to assist degradation of DRiPs. However, whether BAG6 is involved in granulostasis is unknown. We report that BAG6 is not recruited into SGs induced by different types of stress, nor does it affect SG dynamics. BAG6 also does not replace BAG3's function in SG granulostasis. We show that BAG3 and BAG6 target different subsets of DRiPs, and BAG3 binding to DRiPs is mediated by HSPB8 and HSP70. Our data support the idea that SGs are sensitive to BAG3-HSP70-bound DRiPs but not to BAG6-bound DRiPs. Additionally, only BAG3 is strongly upregulated in the stress recovery phase, when SGs dissolve. These data exclude a role for BAG6 in granulostasis and point to a more specialized function in the clearance of a specific subset of DRiPs.

Keywords BAG proteins · Co-chaperones · Newly synthesized proteins · Protein clearance · Stress granule dynamics

Introduction

Stress granules (SGs) are ribonucleoprotein (RNP) granules that contain translationally repressed mRNAs and are induced by different types of stresses such as high temperature, oxidative stress, osmolarity changes, and viral infection (Anderson and Kedersha 2002a). SGs are thought to assemble by liquid-liquid phase separation (LLPS), a process by which a solution of components separates into a dense phase (or condensate) that stably coexists with a dilute phase (Molliex et al. 2015; Patel et al. 2015). SG condensates have liquid-like properties and are highly dynamic: their assembly and disassembly occur rapidly, within minutes rather than hours. The components that condense into SGs are mRNAs released by disassembling polysomes, RNA-binding proteins (RBPs), such as Ras GTPase-activating protein-binding protein (G3BP) and T cell intracytoplasmic antigen (TIA-1), and a large variety of

✉ Serena Carra
serena.carra@unimore.it

[1] Centre for Neuroscience and Nanotechnology, Department of Biomedical, Metabolic and Neural Sciences, University of Modena and Reggio Emilia, Modena, Italy

[2] Max Planck Institute of Molecular Cell Biology and Genetics, 01307 Dresden, Germany

[3] Genomic and post-Genomic Center, IRCCS Mondino Foundation, Via Mondino 2, 27100 Pavia, Italy

[4] Biotechnology Center (BIOTEC), Center for Molecular and Cellular Bioengineering (CMCB), Technische Universität Dresden, Tatzberg 47/49, 01307 Dresden, Germany

[5] Department of Neuroscience, St. Agostino Estense Hospital, Azienda Ospedaliero Universitaria di Modena, Modena, Italy

additional proteins, such as translation factors, signaling molecules, and protein kinases (Protter and Parker 2016). SG assembly can be triggered by two pathways: phosphorylation and inactivation of the key translation initiation factor eIF2 (Anderson and Kedersha 2002b; Sidrauski et al. 2015) or, alternatively, inactivation of other translation initiation factors, such as eIF4A or eIF4G (Farny et al. 2009; Grousl et al. 2009; Knutsen et al. 2015). Functionally, SGs have been suggested to regulate signaling pathways by sequestering signaling molecules such as raptor and mTOR (Kedersha et al. 2013; Thedieck et al. 2013). SGs have also been proposed to protect certain mRNAs from degradation (Decker and Parker 2012; Ivanov et al. 2019).

During the last decade, SGs have received a great deal of attention because their dysfunction has been connected to neurodegenerative diseases such as amyotrophic lateral sclerosis (ALS), frontotemporal dementia (FTD), and inclusion body myopathy (IBM) (Nedelsky and Taylor 2019). Although clinically distinct and heterogeneous, ALS, FTD, and IBM share common pathomechanisms, which include impaired RNA metabolism, formation of aberrant RNP granules, and dysfunctional protein clearance via autophagy (Nedelsky and Taylor 2019; Taylor et al. 2016). Mutations in SG proteins such as TAR-DNA binding protein-43 (TDP-43), fused in sarcoma (FUS), heterogeneous nuclear ribonucleoprotein A1 (hnRNPA1), or TIA-1 and mutations in protein quality control (PQC) factors have been observed in familial forms of these diseases. It has been proposed that these mutations impair the dynamics of RNP granules through protein aggregation, which eventually leads to cell death (Nedelsky and Taylor 2019; Taylor et al. 2016).

There is a great deal of evidence for this model. Mutated RBPs linked to ALS/FTD or IBM change the dynamic behavior of SGs both in vitro and in cells. In vitro, mutant RBPs undergo LLPS but the formed condensates rapidly mature into a solid-like state that is similar to the amyloid-like aggregates found in patient samples. In cells, the mutated forms of these RBPs show enhanced aggregation propensity and, when accumulating inside SGs, they promote the conversion of SGs into a less dynamic, aggregate-like state (Nedelsky and Taylor 2019). These aberrant SGs are recognized by the protein quality control machinery, which targets them for clearance by both the proteasome and the autophagy systems (Buchan et al. 2013; Chitiprolu et al. 2018; Turakhiya et al. 2018). At the same time, ALS-causing mutations have been identified in genes coding for protein quality control factors, such as the molecular chaperone valosin containing proteins (VCP) and the autophagy receptor p62/sequestosome 1 (SQSTM1) (Fecto et al. 2011; Johnson et al. 2010).

The conversion of SGs into an aberrant state can also be triggered by the accumulation of misfolded proteins, in particular newly synthesized defective ribosomal products (DRiPs), which are prematurely terminated polypeptides that are released by disassembling polysomes, immediately prior to SG assembly (Ganassi et al. 2016; Mateju et al. 2017; Turakhiya et al. 2018). DRiPs are highly heterogeneous and include prematurely terminated proteins that arise from errors in protein biogenesis, products of non-canonical translation, and mistranslation from initiation on downstream AUG codons, non-AUG start codons, and stop codon read-through (Schubert et al. 2000). DRiPs are unable to reach their native state and are recognized by the protein quality control system and cleared by proteasomes or the autophagy machinery (Qian et al. 2006; Schubert et al. 2000). The molecular chaperone VCP and also the chaperones Hsc70 and HSP70 form a first line of defense against DRiPs and target them for disposal with assistance by proteasomes and SQSTM1 (Defenouillere et al. 2013; Frydman 2001; Hartl and Hayer-Hartl 2002; Schubert et al. 2000; Szeto et al. 2006; Verma et al. 2013).

Recent evidence indicates that DRiPs have a tendency to accumulate inside SGs, promoting the maturation of SGs into an aberrant aggregate-like state (Ganassi et al. 2016; Mateju et al. 2017; Seguin et al. 2014; Turakhiya et al. 2018). In agreement with their role in the quality control of DRiPs, VCP (Buchan et al. 2013; Seguin et al. 2014; Turakhiya et al. 2018) and the HSPB8-BAG3-HSP70 chaperone complex (Ganassi et al. 2016) have been shown to prevent or reduce DRiP accumulation inside SGs. HSPB8 is an ATP-independent small HSP that binds to a large variety of misfolded and aggregation-prone proteins and keeps them in a state competent for further processing by HSP70, which is an ATP-dependent chaperone (Carra et al. 2008a; Minoia et al. 2014). BAG3 (Bcl2-associated athanogene 3) is a nucleotide exchange factor that acts as a co-chaperone of Hsc70/HSP70 and regulates its activity (Takayama and Reed 2001). The HSPB8-BAG3-HSP70 chaperone complex also interacts with SQSTM1 and has been shown to facilitate autophagy-mediated clearance of aggregation-prone proteins, including DRiPs (Gamerdinger et al. 2011; Ganassi et al. 2016; Guilbert et al. 2018). As such, the HSPB8-BAG3-HSP70 chaperone complex limits the accumulation of DRiPs inside SGs, contributing with VCP to maintain their dynamic liquid-like state, a process that has been referred to as granulostasis (Ganassi et al. 2016). However, given the diversity of DRiPs, it is not known whether specific subsets of DRiPs preferentially accumulate inside SGs and affect their dynamics. Recent findings show that, under proteotoxic stress conditions, DRiPs can also be targeted to other types of condensates, such as nucleoli and PML nuclear bodies (Mediani et al. 2019), besides accumulating in cytoplasmic foci and SGs (Ganassi et al. 2016; Mateju et al. 2017; Szeto et al. 2006). Together these data strongly support the idea that specific subsets of DRiPs, which are handled by different types of PQC machinery, would differentially affect several types of condensates.

BAG3 is a member of the BAG (Bcl-2 associated athanogene) family of proteins, which includes 6 members

in humans (BAG1-6) (Takayama and Reed 2001). All these proteins share the conserved BAG domain and act as Hsc70/HSP70 co-chaperones (Takayama and Reed 2001). However, while BAG3 targets HSP70-bound substrates for clearance by autophagy, through interaction with SQSTM1 (Carra et al. 2008a; Gamerdinger et al. 2011; Minoia et al. 2014), BAG1 mainly targets HSP70-bound substrates for clearance by the proteasome, through interaction with the E3 ubiquitin ligase CHIP (Demand et al. 2001). Similar to BAG1, BAG6 has been linked to proteasome-mediated degradation of proteins, including DRiPs (Minami et al. 2010). However, in contrast to other BAG members, BAG6 was shown to interact with the 26S proteasomal complex and polyubiquitinated proteins (Minami et al. 2010). Intriguingly, BAG6 directly interacts with polyubiquitinated proteins via its N-terminal 471 amino acids (N471) and not via the BAG domain (which recruits HSP70), nor via the ubiquitin-like (UBL) domain (Minami et al. 2010). This is in sharp contrast to other BAG proteins, such as BAG3, for which the binding to polyubiquitinated substrates is not direct but mediated by HSP70 (Takayama and Reed 2001). Experiments performed to identify the origin of polyubiquitinated proteins bound by BAG6 indicate that BAG6 associates with newly synthesized proteins, in particular newly synthesized transmembrane proteins and ER-derived proteins, as well as to DRiPs, to favor their proteasome-mediated clearance (Claessen and Ploegh 2011; Kadowaki et al. 2015; Kawahara et al. 2013; Leznicki et al. 2010; Minami et al. 2010).

Here, we investigate whether BAG6 participates in granulostasis by preventing the accumulation of DRiPs inside SGs. Our data demonstrate that BAG6 is not recruited inside SGs and that BAG6 depletion does not affect SG dynamics, nor it can functionally replace BAG3, excluding a role for BAG6 in granulostasis. This functional difference relies on the fact that BAG3 and BAG6 target different subsets of DRIPs that have different subcellular destinations. Our data support the idea that the subset of DRiPs directly bound by HSP70 and cleared with the assistance of BAG3 is the one that tends to accumulate inside SGs, thereby impairing SG dynamics. Additionally, only BAG3 is significantly upregulated in the stress recovery phase, when SGs dissolve, in primary fibroblasts from healthy donors.

Material and methods

Cell culture and transfection

HeLa cells were grown in Dulbecco's modified Eagle's medium (DMEM) high glucose (4.5 g/L) (Euroclone) at 37 °C and 5% CO_2 supplemented with L-glutamine (2 mM), penicillin/streptomycin (100 U/mL), and 10% fetal bovine serum (Corning). ON-TARGETplus BAG6 siRNA, ON-TARGETplus BAG3 siRNA, and control siGENOME Non-Targeting control siRNAs were from Dharmacon. cDNA encoding for His-BAG3, His-BAG3-ΔBAG, and His-BAG3-ΔB8 were previously described (Carra et al. 2008b); the cDNA encoding for V5-HSP70 was a kind gift from Dr. H.H. Kampinga (Hageman and Kampinga 2009). Cells were transfected using Lipofectamine 2000 (Life Technologies) according to the manufacturer's instructions.

Human skin fibroblasts were generated from skin biopsies of three healthy donors. All donors provided written informed consent for the collection of skin biopsies and the use of skin fibroblast lines for research purposes. Human fibroblasts were cultured in DMEM medium with high glucose (4.5 g/L) (Euroclone), supplemented with L-glutamine (2 mM), penicillin/streptomycin (100 U/mL), antibiotic/antimycotic solution stabilized (100 U/ml), and 10% fetal bovine serum, at 37 °C with 5% CO_2.

Protein extraction and Western blotting

To extract total proteins, cells were lysed in Laemmli buffer containing 2% SDS and homogenized by sonication. Protein samples were boiled for 3 min at 100 °C, reduced with β-mercaptoethanol, and separated by SDS-PAGE. Separated proteins were transferred onto nitrocellulose membranes. Membranes were blocked with 3% BSA-Tris-buffered saline (TBS) with Tween 20 (0.01%) for 1 h at room temperature, then were incubated for 16 h at 4 °C with the following antibodies: puromycin (Merck), BAG6 (Abcam), home-made rabbit antibodies against BAG3 and HSPB8 (Carra et al. 2008a), HSPA1A (HSP70) (StressMarq Biosciences), ubiquitin (Dako), and TUBA4A (Sigma-Aldrich). Blots were then incubated with HRP-conjugated anti-mouse and anti-rabbit antibodies (GE-Healthcare). After washes, bands were detected by chemiluminescence using Westar ECL reagents (Cyanagen). Images were acquired with ChemiDoc Imaging System (Bio-Rad).

Preparation of samples for confocal microscopy analysis

Cells were grown on glass coverslip coated with poly-L-lysine. After treatments, cells were washed with cold PBS 1× (Euroclone), fixed with 3.7% formaldehyde in PBS 1× for 9 min at room temperature, followed by permeabilization with cold acetone for 5 min at − 20 °C. Cells were blocked in 3% BSA in PBS 1× supplemented with 0.1% Triton X-100 for 1 h at room temperature. After blocking, cells were incubated for 16 h at 4 °C with the following primary antibodies: home-made rabbit polyclonal BAG3 antibody (Carra et al. 2008a), BAG6 (Abcam), G3BP (BD-Bioscience), and TIA-1 (Santa Cruz Biotechnology). Fixed cells were then incubated with fluorescent-conjugated secondary antibodies (Thermo

Scientific) and DAPI (Sigma-Aldrich) for 1 h at room temperature.

Labeling of nascent peptides with puromycin or op-PURO

Analysis of nascent proteins in whole-cell lysates: cells were treated with puromycin dihydrochloride (5 μg/ml; Sigma-Aldrich) for 10 min at 37 °C. For recovery experiments, cells were washed three times and incubated for the indicated time points in drug-free medium. Cells were lysed in Laemmli buffer and subsequently processed for Western blot analysis with the indicated antibodies.

Analysis of nascent proteins by confocal microscopy: newly synthesized proteins were labeled by incubating the cells with 25 μM O-propargyl-puromycin (OP-puro) (Jena Bioscience) for the indicated time points; where indicated, cells were co-treated with MG132 (Sigma-Aldrich) and VER-155008 (Sigma-Aldrich). Treated cells were fixed with cold methanol for 5 min at − 20 °C. OP-puro-labeled peptides were detected by click chemistry as previously described (Seguin et al. 2014).

Ni-NTA agarose pull-down

HeLa cells were transfected with cDNA encoding for His-tagged BAG3: His-BAG3, His-BAG3-ΔBAG, and His-BAG3-ΔB8 (Carra et al. 2008b; Fuchs et al. 2009) or V5-HSP70 (Hageman and Kampinga 2009) or an empty vector. Twenty-four hours post-transfection, cells were scraped and homogenized in lysis buffer (20 mM Tris/HCl pH 7.4, 2.5 mM MgCl2, 3% (v/v) glycerol, 0.5% NP40 (Nonidet P40), 150 mM NaCl, 10 mM imidazole, 1 mM DTT and 1× complete protease inhibitor cocktail (Roche)). The cell lysates were centrifuged at 14.000*g* at 4 °C to pellet NP40 insoluble proteins. His-BAG3 proteins were purified from NP40-soluble lysates using Ni-NTA agarose beads (Qiagen). After 1 h of incubation at 4 °C, the Ni-NTA beads were washed several times with a washing buffer enriched in imidazole (20 mM Tris/HCl pH 7.4, 2.5 mM MgCl2, 3% (v/v) glycerol, 0.5% NP40, 300 mM NaCl, 20 mM imidazole, and 1× complete protease inhibitor cocktail (Roche)). The proteins bound to the beads were recovered by boiling in 2% SDS sample buffer and the fractions were then separated by SDS-PAGE, followed by Western blotting with the indicated antibodies.

Analysis of stress granule sensitivity to RNase

HeLa cells were seeded on glass coverslip coated with poly-L-lysine (Sigma-Aldrich). After 24 h, cells were treated with MG132 (Sigma-Aldrich) to induce stress granules. Cells were either immediately fixed (before RNase) or quickly washed with PBS 1× containing Triton X-100 (0.05%), followed by washing with PBS 1×. Cells were then incubated for 30 min at room temperature with the RNAse buffer (0.2 mg/ml RNAse solution in PBS 1×; Sigma-Aldrich). After RNase treatment, cells were fixed as previously described and subjected to immunofluorescence analysis, with the indicated antibodies.

Analysis of stress granule composition number and size with high content imaging-based assays

Confocal images were obtained using a Leica SP2 and a Leica SP8 AOBS system (Leica Microsystems) and a 63× oil immersion lens. Enrichment of DRiPs and BAG6 inside SGs, area, and number of SGs were analyzed using the Scan^R Analysis software (Olympus). SGs were segmented based on G3BP or TIA-1 signal using edge detection algorithm and the mean fluorescence intensity of the protein of interest (DRiPs or BAG6) was measured in each segmented SG, as well as in an area surrounding each SG. The relative enrichment of DRiPs or BAG6 in individual SGs was calculated as a ratio of mean fluorescence intensity inside the SG divided by the mean intensity in the region surrounding the SG. The values obtained were plotted as column graphs; the fraction of SGs with enrichment > 1.5 is shown.

RNA extraction and RT-qPCR analysis

Human fibroblasts were seeded and when optimal cell density was reached, cells were either left untreated or treated with sodium arsenite 0.5 mM (Carlo Erba Reagents) for 45 min to induce SGs. Then cells were either collected immediately after arsenite treatment or allowed to recover in drug-free medium for 4 h. Total RNA was isolated from untreated and treated human fibroblasts using TRIzol reagent (Zymo research). Total RNA was purified with RNA Clean & Concentrator Zymo kit (Zymo Research) according to the manufacturer's instructions. 0.25 μg of RNA was reverse transcribed using Maxima First-strand cDNA Synthesis Kit with dsDNase (Thermo Fisher) according to the manufacturer's instructions. PCR amplification was performed using Maxima SYBR Green qPCR Master Mix polymerase (Thermo Fisher). The expression levels of human BAG3 and BAG6 mRNAs were determined using CFX96 Touch Thermal cycler (Bio-Rad) in combination with SYBR green master mix. Data were normalized against RPL0, which was used as a housekeeping gene. The primers used are as follows (Eurofins-Genomics): BAG3 For (TCCTGGACACATCCCAATTC); BAG3 Rev (TCTCTTCTGTAGCCACACTC); BAG6 For (TTGGTGAAGACCTTGGACTC); BAG6 Rev (TTCAGATGGGATGCTGACAG); RPL0 For (TTAAACCCTGCGTGGCAATCC); RPL0 Rev (CCACATTCCCCCGGATATGA). qPCR was performed as follows: one cycle of denaturation (95 °C for 3 min); 40 cycles of amplification (95 °C for 10 s, 60 °C for 30 s). A

triplicate of each sample was analyzed with Bio-Rad CFX Manager 3.1 (Windows 7.0).

Statistical analyses

Statistical analyses were performed using a one-way ANOVA, followed by Bonferroni-Holm post-hoc test for comparisons between three or more groups; for comparisons between two groups, statistical analyses were performed using Student's *t*-test. The software used for statistical analysis is Daniel's XL Toolbox.

Results

BAG6 colocalizes with DRiPs and promotes their clearance

We previously reported that BAG3 colocalizes with nascent misfolded proteins generated by treating the cells with puromycin or its analog OP-puro; we also found that BAG3 depletion decreases the ability of the cells to clear puromycylated proteins, suggesting a role for BAG3 in their clearance (Ganassi et al. 2016). Like BAG3, BAG6 has been reported to interact with puromycylated nascent chains; BAG6 also binds to the 26S proteasomes, thereby facilitating the clearance of the bound nascent proteins (Minami et al. 2010). By confocal microscopy, we show that both BAG3 and BAG6 partially colocalize with OP-puro-labeled nascent chains that accumulate in cytoplasmic and nuclear puncta in cells treated with OP-puro alone or co-treated with the proteasome inhibitor MG132 (DRiPs; Fig. 1a).

To determine whether BAG6 plays a role in the clearance of puromycylated proteins, we compared the amount of puromycylated proteins in the presence or absence of BAG6. BAG6-proficient and BAG6-deficient HeLa cells were treated with puromycin for 45 min, followed by recovery in drug-free medium for 13 h, to allow DRiP clearance. BAG6 depletion led to a small, but significant, accumulation of puromycylated nascent chains, compared with control cells (Fig. 1b). This result confirms that, similar to BAG3 (Ganassi et al. 2016; Meriin et al. 2018), BAG6 participates in the degradation of DRiPs in HeLa cells.

BAG6 is not recruited into stress granules and is not required for their dissolution

Exposure of mammalian cells to environmental stressors induces the assembly of SGs (Kedersha and Anderson 2002).

We previously reported that BAG3, but not BAG1, was recruited into SGs (Ganassi et al. 2016). It was also previously reported that BAG6 is not recruited into arsenite-induced SGs in U2OS cells (Alexander et al. 2018). SGs induced by different types of stress are not uniform and differ in their composition

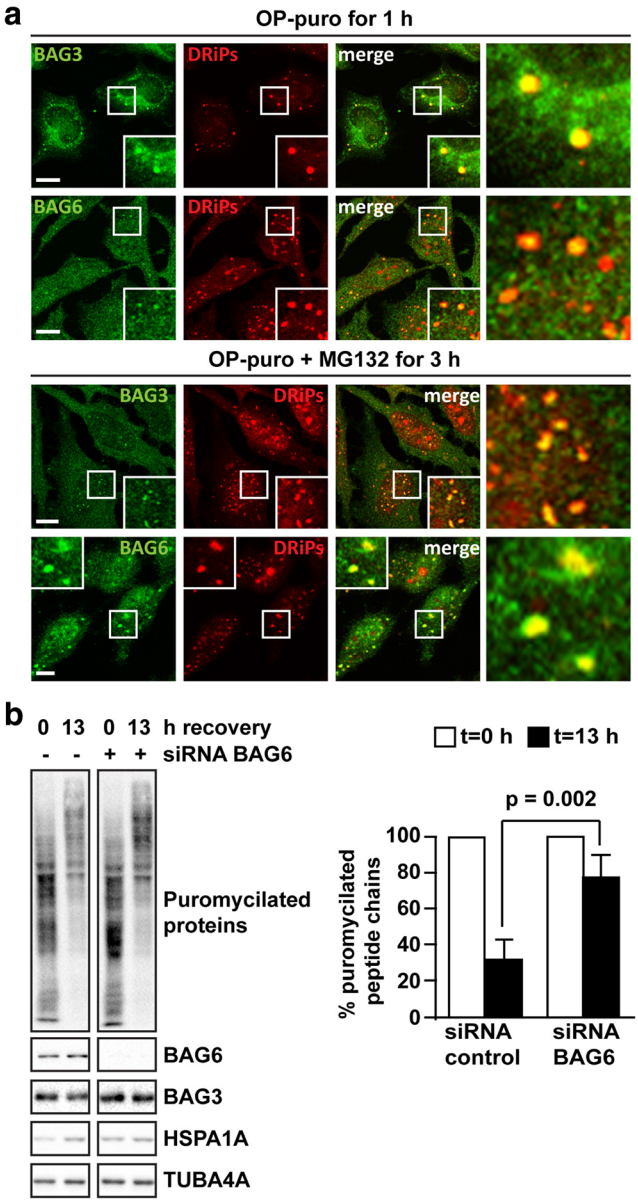

Fig. 1 BAG6 colocalizes with DRiPs and participate in their clearance. **a** HeLa cells were treated with OP-puro (25 μM) for 1 h or with OP-puro (25 μM) and MG132 (20 μM) for 3 h. Cells were fixed and then subjected to immunofluorescence using specific antibodies for BAG3 or BAG6. OP-puro-labeled nascent chains were visualized by click chemistry with Alexa594-Azide (DRiPs). Scale bars = 10 μm. **b** HeLa cells were lipofected for 72 h with siRNA non-targeting control or against BAG6. Then, cells were incubated with puromycin 10 μg/ml for 45 min, followed by recovery in drug-free medium for 13 h. Proteins were extracted from the treated cells and subjected to SDS-PAGE, followed by immunoblotting using the indicated antibodies. Quantitation of the percentage of puromycylated peptide chains is reported. $n = 3$, +/− SEM, $p = 0.002$

(Aulas et al. 2017). Thus, we verified the subcellular localization of BAG6 in HeLa cells exposed to different types of stressors that induce SG formation, namely, sodium arsenite, heat shock, and inhibition of the proteasome with MG132 (Kedersha and Anderson 2002; Mazroui et al. 2007). SGs were

labeled with an antibody for G3BP, a well-known SG component (Tourriere et al. 2003). BAG6 was generally excluded from SGs induced by arsenite, heat shock, or proteasome inhibition and showed a diffuse distribution, both in the cytoplasm and nucleus (Mock et al. 2017), under all condition tested (Fig. 2a). In cells treated with MG132 and OP-puro, BAG6 did not colocalize with cytosolic SGs (Fig. 2b, upper panel). The majority of these SGs rapidly dissolve during the recovery phase (Ganassi et al. 2016) and are not enriched for DRiPs (Fig. 2b, upper panel). To induce aberrant SGs that contain high levels of DRiPs (Ganassi et al. 2016), we co-treated cells with MG132 and the HSP70 ATPase inhibitor VER-155008 (VER). However, BAG6 did not colocalize with aberrant DRiP-containing SGs (Fig. 2b, lower panel). Thus, we conclude that unlike BAG3, BAG6 is not recruited into aberrant SGs.

Next, we investigated whether BAG6 may play an indirect role in regulating SG dynamics, for example by promoting DRiP clearance. We depleted BAG6 levels with specific siRNAs and determined SG dissolution time, enrichment for DRiPs, and resistance to RNase digestion, all parameters that were previously demonstrated to affect the conversion of SGs into an aberrant state (Ganassi et al. 2016). BAG6 depletion did not delay SG dissolution upon prolonged treatment with MG132 (Fig. 3a) (Ganassi et al. 2016; Mazroui et al. 2007), nor did it cause a significant accumulation of DRiPs inside SGs (Fig. 3b); actually, BAG6 depletion slightly reduced the levels of DRiPs inside SGs (Fig. 3b). This is in contrast to BAG3-deficient cells, which failed to dissolve SG upon prolonged treatment with MG132, causing a delay in the restoration of normal translation rates (Ganassi et al. 2016). In addition, both in control and BAG6-depleted cells the majority of SGs were sensitive to RNase digestion, indicating that SGs did not convert into proteinaceous aggregates (Fig. 3c, d). Importantly, BAG6 depletion did not affect the expression level, nor the MG132-mediated upregulation of BAG3 and HSP70 (Fig. 3e). SG assembly occurs when polysomes dissociate and the translation is inhibited; conversely, SG disassembly correlates with the restoration of translation, which can be monitored by measuring the incorporation of puromycin into newly synthesized polypeptides (Anderson and Kedersha 2002b; Ganassi et al. 2016). Both in control and BAG6-depleted cells puromycin incorporation strongly decreased after 3 h of treatment with MG132, when the SG response is maximal; instead, puromycin incorporation was partly restored after 6–8 h of treatment with MG132, when SGs disassemble, both in control and BAG6-depleted cells (Fig. 3e). We conclude that BAG6 depletion does not change the composition, dynamics, and biochemical properties of SGs.

BAG6 does not replace BAG3 function at the level of stress granules

The observation that only depletion of BAG3, but not of BAG6, affects SG composition and dynamics is intriguing, considering that both BAG3 and BAG6 promote the clearance of newly synthesized proteins and DRiPs (Ganassi et al. 2016;

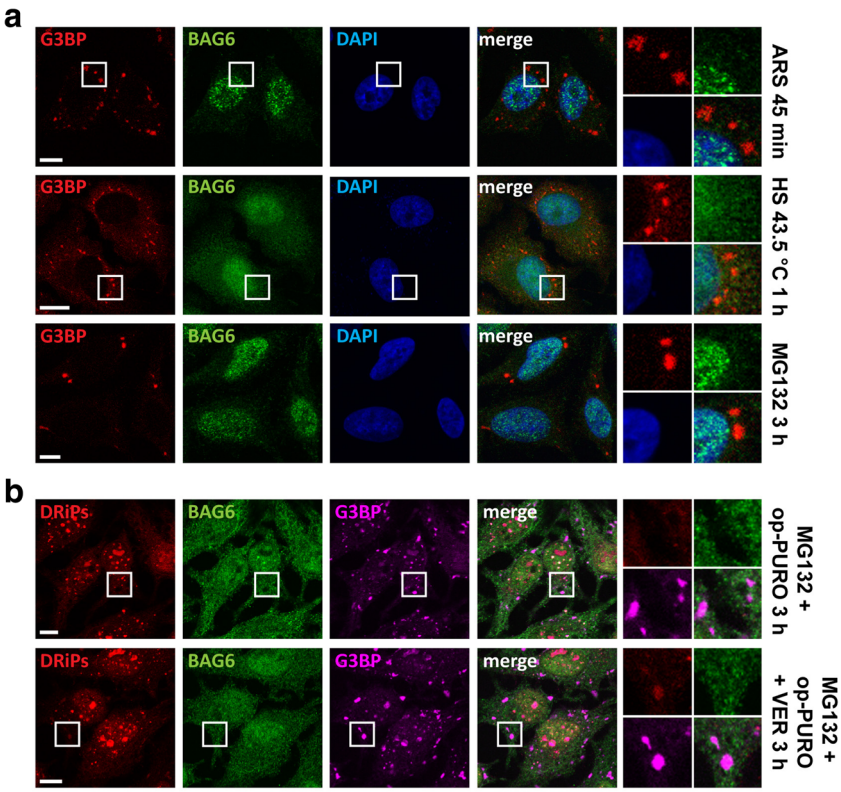

Fig. 2 BAG6 is not recruited inside stress granules. **a** HeLa cells were treated with arsenite 0.5 mM for 45 min or heat shock (HS) at 43.5 °C for 1 h or MG132 20 μM for 3 h. Cells were fixed and subjected to immunofluorescence using antibodies specific for the SG protein G3BP and BAG6. Scale bars = 10 μm. **b** HeLa cells were treated with MG132 20 μM and OP-puro 25 μM for 3 h, where indicated HSP70 ATPase activity was blocked using 40 μM VER-155008. Cells were fixed and subjected to immunofluorescence using specific antibodies for G3BP and BAG6. OP-puro-labeled nascent chains were visualized by click chemistry with Alexa594-Azide. Scale bars = 10 μm

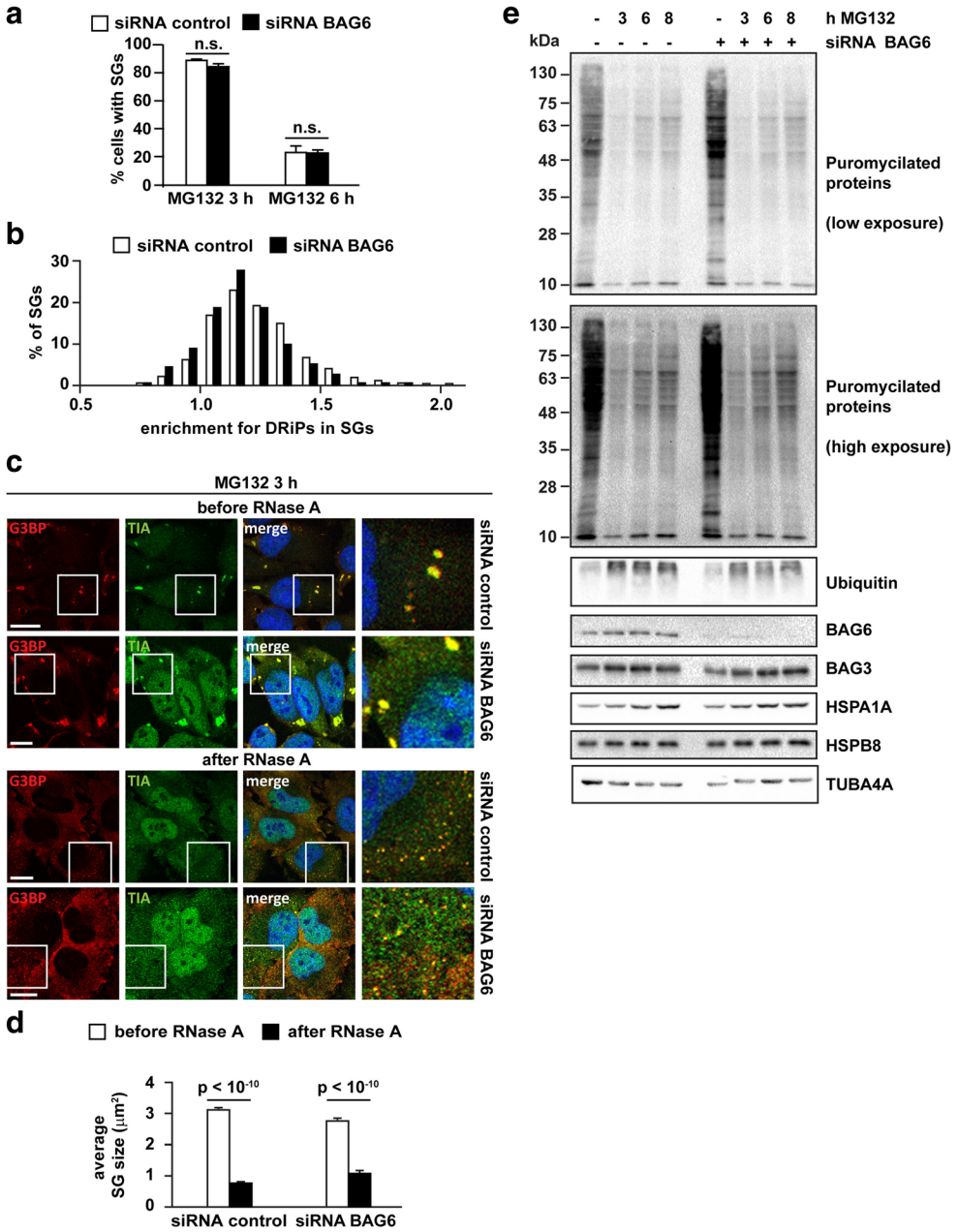

Fig. 3 BAG6 depletion does not affect SG dynamics. **a** HeLa cells were lipofected for 72 h with siRNA non-targeting control or against BAG6. Cells were exposed to MG132 (20 μM) for 3 or 6 h, fixed, and subjected to immunostaining with antibodies specific for the SG proteins TIA1 (TIA) and G3BP. The percentage of cells with SGs is reported; from 342 to 589 cells were counted/sample; $n = 3$, +/− SEM. **b** Quantitation of DRiP enrichment inside SGs in control or BAG6-depleted cells. SGs were induced with MG132 20 μM and OP-puro 25 μM for 3 h. Automated imaging and SG segmentation is based on G3BP signal. Number of SGs counted: 1188 (siRNA control); 855 (siRNA BAG6); $p = 10^{-10}$. **c** SGs were induced in control or BAG6-depleted cells. 3 h after treatment with MG132, cells were either immediately fixed or treated with RNAse A for 30 min at RT prior to fixation. Representative pictures of TIA and G3BP positive SGs before and after RNAse digestion. Scale bars = 10 μm. **d** Quantitation of SG size (μm^2) before and after RNase treatment in cells from **c**. $p < 10^{-10}$, +/− SEM. Number of SGs counted: 1330 (siRNA control before RNase); 1918 (siRNA control after RNase); 1020 (siRNA BAG6 before RNase); 1350 (siRNA BAG6 after RNase). **e** HeLa cells were lipofected for 72 h with siRNA non-targeting control or against BAG6. Cells were exposed to MG132 (20 μM) for 3, 6, or 8 h. Puromycin 5 μg/ml was added during the last 15 min of treatment, prior to protein extraction. Samples were processed for Western blot

Meriin et al. 2018; Minami et al. 2010). This may be due to several reasons, one possibility being differences in expression levels. BAG3 is strongly upregulated upon stress such as prolonged proteasome inhibition and its depletion may hamper the cell stress response, leading to aberrant SG accumulation. We thus determined whether BAG6 expression is induced upon proteasome inhibition. Indeed, BAG6 was moderately upregulated upon treatment of cells with MG132 for 6 h (Fig. 4a).

BAG3 has a binding affinity for HSP70 much higher than other BAG members (Rauch and Gestwicki 2014), suggesting that it may compete with other BAG proteins for HSP70 binding and has a specific function in the cellular response to proteasome inhibition. We wondered whether there are any functional redundancies between BAG6 and BAG3 and whether BAG6 can functionally rescue cells that lack BAG3. To address this question, we depleted BAG3 with a specific siRNA and analyzed BAG6 recruitment into SGs that were induced using MG132 alone or combined with VER. We found no evidence for BAG6 accumulation inside SGs in BAG3 depleted cells compared with control cells (Fig. 4b, c). These data exclude a role for BAG6 in granulostasis, also as a potential helper of BAG3.

We next sought to further understand the differential impact of BAG3 and BAG6 on SG dynamics. It is currently unknown whether specific subsets of DRiPs preferentially accumulate inside SGs, thereby impairing their dynamics. So far, inhibition of HSP70 and VCP and depletion of the HSPB8-BAG3 subcomplex have been shown to enhance DRiP accumulation inside SGs, suggesting that SGs may be particularly sensitive to DRiPs bound to the HSPB8-BAG3-HSP70 complex and to VCP (Buchan et al. 2013; Ganassi et al. 2016; Mateju et al. 2017; Seguin et al. 2014; Turakhiya et al. 2018). Significantly, BAG6 can directly bind to 26S proteasomes and associates with puromycilated proteins in an HSP70-independent manner (Minami et al. 2010). By contrast, BAG3 binding to ubiquitylated and puromycilated proteins is dependent on Hsc70/HSP70 binding via the BAG domain (Gentilella and Khalili 2011; Minoia et al. 2014). The small heat shock protein HSPB8 has also been suggested to present misfolded proteins, including ubiquitinated proteins and DRiPs, to the BAG3-HSP70 subcomplex for further processing (Ganassi et al. 2016; Guilbert et al. 2018). We thus determined whether two variants of BAG3 unable to bind to HSPB8 (His-BAG3-ΔB8) or Hsc70/HSP70 (His-BAG3-ΔBAG) still associate with puromycilated proteins (Carra et al. 2008b; Fuchs et al. 2009). HeLa cells were transfected with cDNAs encoding wild-type BAG3 (His-BAG3), His-BAG3-ΔB8, or His-BAG3-ΔBAG and the associated protein complexes were purified using Ni-NTA agarose beads. Deletion of the HSPB8-binding domain reduced the ability of BAG3 to interact with HSPB8 (Fig. 4d), and deletion of the BAG domain abrogated BAG3 binding to HSP70 (both endogenous and overexpressed V5-tagged HSP70), while leaving unaffected BAG3 binding to HSPB8 (Fig. 4e). Next, we treated His-BAG3, His-BAG3-ΔB8, or His-BAG3-ΔBAG expressing cells with puromycin to label nascent chains prior to purification with Ni-NTA. Deletion of either the HSPB8 or HSP70 binding domains decreased the amount of puromycilated proteins associated with BAG3 (Fig. 4f). Thus, we conclude that BAG3 associates with puromycilated proteins that are presented by chaperones such as HSPB8 or HSP70. This is consistent with the idea that BAG6 and BAG3 bind to different pools of DRiPs and suggests that SGs are sensitive to DRiPs targeted by Hsc70/HSP70 or HSPB8, but not to DRiPs that associate with BAG6 in a direct, HSP70-independent manner.

BAG3, but not BAG6, is strongly upregulated during the SG dissolution phase in fibroblasts from healthy individuals

Conversion of SGs into an aggregate-like state because of the accumulation of DRiPs or ALS-associated mutations in RBPs has been reported in different cells types, from immortalized mammalian cells such as HeLa cells to iPSC-derived neurons and patient-derived fibroblasts (Ganassi et al. 2016; Marrone et al. 2018; Mateju et al. 2017). Disassembly of these SGs is facilitated by HSP70s, which act in concert with other chaperones and co-chaperones such as HSPB1, HSPB8, and BAG3 (Ganassi et al. 2016). Importantly, experiments performed in immortalized cancer cell lines demonstrated that these chaperones are upregulated during stress to cope with the increasing amounts of stress-induced misfolded proteins (Ganassi et al. 2016; Minoia et al. 2014; Wang et al. 2008). However, it is unclear whether BAG3 is also induced in primary cells. We analyzed the mRNA levels of BAG3 and BAG6 in fibroblasts from 3 healthy donors. The fibroblast lines were either left untreated, exposed to sodium arsenite to induce SGs, or exposed to sodium arsenite and a 4 h recovery in drug-free medium to allow for SG dissolution. qPCR analyses showed that BAG3 mRNA is strongly upregulated in the recovery phase, when SGs dissolve (Fig. 5a). By contrast, the expression levels of BAG6 were not induced in all fibroblast lines analyzed (Fig. 5b). This further supports the notion that these two co-chaperones exert distinct functions and that in contrast to BAG6, BAG3 is specifically upregulated in the SG dissolution phase to promote granulostasis (Fig. 6).

Discussion

DRiPs represent the major source of misfolded proteins in cells (Schubert et al. 2000); they are cleared with the assistance of chaperones and degradation systems (proteasomes and autophagy) (Balchin et al. 2016; Schubert et al. 2000; Verma et al. 2013). When clearance fails, DRiPs assemble into cytoplasmic aggregates outside of condensates or they accumulate in condensates, such as cytoplasmic SGs, but also nucleoli and PML nuclear bodies (Ganassi et al. 2016; Mediani et al. 2019). This can cause the conversion of condensates into an aggregated, amyloid-like state, thus affecting their dynamics and functionality (Ganassi et al. 2016; Mediani et al. 2019). Non-dynamic forms of condensates have been

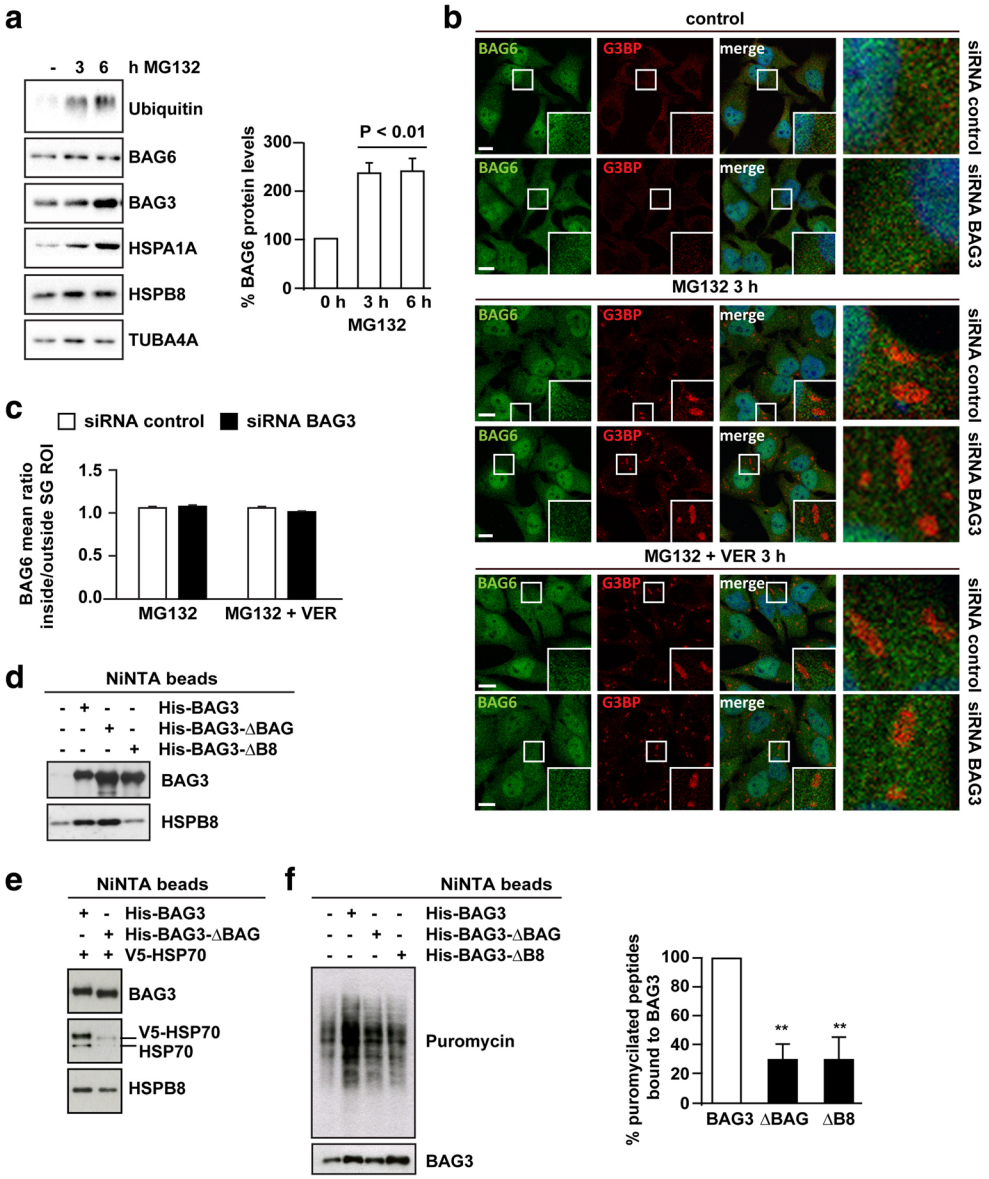

Fig. 4 BAG6 does not replace BAG3 in granulostasis and is not recruited inside stress granules in BAG3-depleted cells. **a** HeLa cells were exposed to MG132 20 μM for 3 or 6 h and protein extracts were prepared and subjected to immunoblotting to measure the expression levels of BAG3, BAG6, HSPB8, and HSPA1A. Quantitation of BAG6 protein levels is reported; $n = 3$, +/− SEM. **b** HeLa cells were lipofected for 72 h with siRNA non-targeting control or against BAG3. Cells were either left untreated (control) or exposed to MG132 (20 μM) alone or with VER-155008 (40 μM) for 3 h, fixed, and subjected to immunostaining with antibodies specific for BAG6 and the SG protein G3BP. Scale bars = 10 μm. **c** Quantitation of BAG6 mean ratio inside/outside SG ROI in cells from **b**. Number of SGs counted: 920 (siRNA control MG132); 1341 (siRNA control MG132 + VER); 419 (siRNA BAG3 MG132); 1619 (siRNA BAG3 MG132 + VER). **d** HeLa cells were transfected with cDNAs encoding for His-BAG3, His-BAG3-ΔBAG, His-BAG3-ΔB8, or empty vector. Twenty-four hours post-transfection, the NP-40 soluble fractions were subjected to Ni-NTA purification, and beads were processed for Western blotting using anti-BAG3 and anti-HSPB8 antibodies. **e** HeLa cells were transfected with cDNAs encoding for His-BAG3, His-BAG3-ΔBAG, or V5-HSP70. Twenty-four hours post-transfection, the NP-40 soluble fractions were subjected to Ni-NTA purification, and beads were processed for Western blotting using BAG3, HSP70, and HSPB8 specific antibodies. **f** HeLa cells were transfected with cDNAs encoding for His-BAG3, His-BAG3-ΔBAG, His-BAG3-ΔB8, or empty vector. Twenty-four hours post-transfection, cells were treated with puromycin (10 μg/ml) for 45 min and then the NP-40 soluble fractions were subjected to Ni-NTA purification and beads were processed for Western blotting using BAG3 and puromycin-specific antibodies. Quantification of the amount of puromycilated proteins pulled-down by His-BAG3, His-BAG3-ΔBAG, or His-BAG3-ΔB8 in three independent experiments is shown; $^{**}p \leq 0.005$, +/− SEM

linked to aging and age-related neurodegenerative diseases, including ALS, FTD, and IBM (Kwon et al. 2014; Lee et al. 2016; Molliex et al. 2015; Murakami et al. 2015; Nedelsky and Taylor 2019; Patel et al. 2015; Qamar et al. 2018; White et al. 2019; Zhang et al. 2019). Thus, identifying factors that help maintain condensate dynamics may offer promising

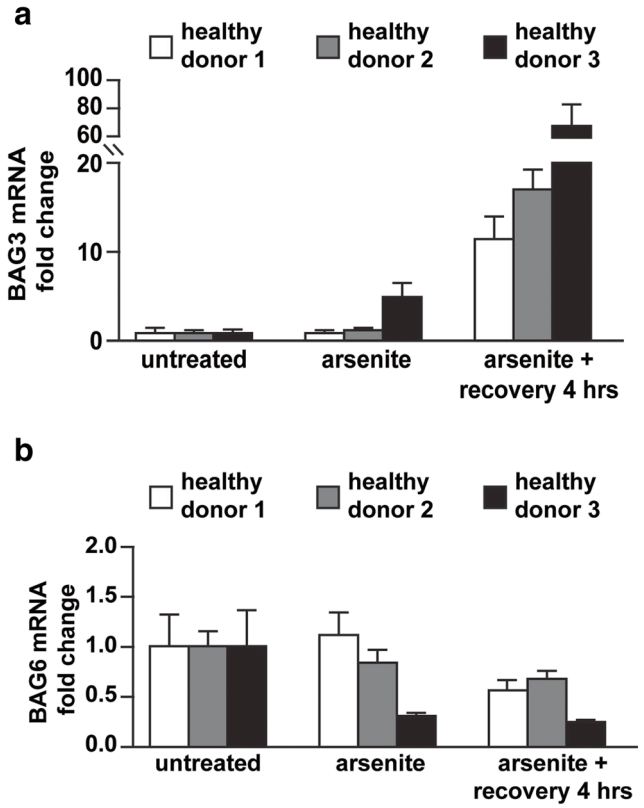

Fig. 5 BAG3, but not BAG6, is induced during the recovery phase after arsenite stress in fibroblasts from healthy donors. **a**, **b** Fibroblast lines derived from 3 healthy donors were cultured for total RNA preparation and analysis of BAG3 and BAG6 mRNA levels. The fibroblast lines were left untreated (untreated), exposed to sodium arsenite (500 μM) for 45 min (arsenite), or allowed to recover for 4 h in drug-free medium after treatment with sodium arsenite (500 μM) for 45 min (arsenite + recovery 4 h). BAG3 (**a**) and BAG6 (**b**) mRNA levels were normalized for RPL0. $n = 3$ independent experiments/condition, +/− SEM

therapeutic avenues for the treatment of these diseases. One group of proteins that can prevent the irreversible accumulation of DRiPs inside condensates are molecular chaperones, including HSP70 and VCP (Ganassi et al. 2016; Mateju et al. 2017; Mediani et al. 2019). In the case of SGs, HSP70 acts in concert with the co-chaperone BAG3 and HSPB8 to target DRiPs for clearance, thereby maintaining SG dynamics, a function referred to as granulostasis (Ganassi et al. 2016) (Fig. 6). Here, we studied whether another BAG family member, BAG6, participates in the process of granulostasis.

Our findings show that both BAG3 and BAG6 promote the clearance of DRiPs. Both BAG3 and BAG6 colocalize with DRiPs in cytoplasmic foci in stressed cells and the depletion of BAG3 and BAG6 decreases the ability of cells to clear puromycilated proteins (Ganassi et al. 2016) (Fig. 1). This establishes a clear function for both BAG3 and BAG6 in the quality control of DRiPs, in line with published literature (Ganassi et al. 2016; Meriin et al. 2018; Minami et al. 2010). In agreement with this, both BAG3 and BAG6 are upregulated following proteasome inhibition, a condition that leads to the accumulation of DRiPs and induces SGs.

We next sought to determine whether BAG3 and BAG6 have similar roles in protecting SGs from converting into a non-dynamic state. Our previous work showed that a fraction of SGs can accumulate DRiPs, an event that is exacerbated by inhibition of HSP70 and by depletion of HSP70 and BAG3, or its partner HSPB8 (Ganassi et al. 2016; Mateju et al. 2017). When SGs accumulate DRiPs, SGs convert into an aberrant state that becomes resistant to digestion with RNase and recruits chaperones such as HSPB1, HSPB8, and BAG3, likely in an attempt to prevent their maturation into irreversible aggregates (Ganassi et al. 2016; Mateju et al. 2017) (Fig. 6). However, in contrast to BAG3, we found no evidence for BAG6 recruitment inside SGs, even in cells where HSP70 was inhibited to enhance the accumulation of DRiPs inside SGs (Fig. 2). Moreover, depletion of BAG6 had no effect on SG dissolution kinetics and did not delay translation restoration during prolonged treatment with MG132, compared with control cells. In addition, BAG6 depletion did not affect the enrichment for DRiPs inside SGs, nor SG sensitivity to digestion with RNase (Fig. 3). BAG6 recruitment inside SGs was also not observed under extreme conditions when BAG3 was depleted and HSP70 was inhibited (Fig. 4). Collectively these results exclude a role for BAG6 in granulostasis and point to a specific function of BAG3. This interpretation is further supported by the finding that BAG3, but not BAG6, is strongly upregulated in the stress recovery phase, the same time period when SGs dissolve (Fig. 5).

Given the heterogeneity of DRiPs and the fact that under stress conditions DRiPs can accumulate in different types of condensates, including SGs, nucleoli, and PML nuclear bodies, these data lead to two important unanswered questions: (1) Are SGs particularly sensitive to a specific subset of DRiPs? (2) Are different subsets of DRiPs handled by specific types of PQC machinery? Our findings are in agreement with the idea that BAG3 and BAG6 target different pools of DRiPs that have different subcellular destinations and/or functions, and, by doing so, they differentially affect the functionality of SGs. This notion is supported by the following considerations. First, BAG6 directly binds to DRiPs in an HSP70 independent manner (Minami et al. 2010) (Fig. 6); by contrast, BAG3 binding to DRiPs is mediated by its interaction with HSP70 and HSPB8, demonstrating that both chaperones present substrates to BAG3 (Fig. 4). The nucleotide exchange factor function of BAG3 may regulate the speed of processing of these substrates by HSP70. Second, BAG6 directly binds to proteasomes and immunoproteasomes, including the thymoproteasomes, which have been identified specifically in thymic epithelial cells, where they play a critical role in the presentation of a unique set of self-peptides that are required for CD8(+) T cell development (Kawahara et al. 2013; Murata et al. 2008). Antigenic peptides are transported to the

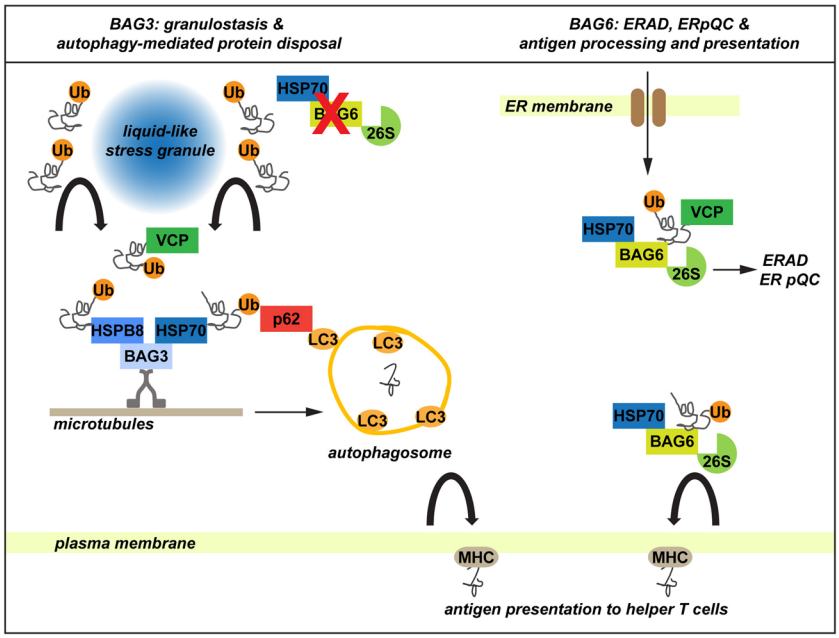

Fig. 6 Distinct functions of BAG3 and BAG6. Upon stress, newly synthesized proteins and DRiPs are released by disassembling polysomes. mRNAs and RBPs are compartmentalized inside stress granules. The VCP, HSPB8, and HSP70 chaperones bind to newly synthesized polyubiquitinated (Ub) proteins, including DRiPs. HSPB8 and HSP70 form a multiprotein complex with BAG3, p62/SQSTM1, and the motor protein dynein that targets DRiPs and polyubiquitinated proteins to LC3-positive autophagosomes for degradation. As such, DRiPs do not accumulate inside stress granules, which maintain their liquid-like properties (Ganassi et al. 2016). BAG6 also binds to HSP70 and polyubiquitinated proteins. However, in contrast to BAG3 (Fig. 4), BAG6 can directly bind to polyubiquitinated proteins and 26S proteasomes (as previously shown by Minami et al. 2010). BAG6 bound to HSP70 and 26S proteasomes is not involved in granulostasis (red cross). Instead, BAG6 targets proteins of the secretory pathway that have failed to insert into the ER to degradation via ERAD and ERpQC, in cooperation with VCP (see Kadowaki et al. 2015; Wang et al. 2011). BAG6 has also been implicated in the processing of antigens that are generated via the degradation of newly synthesized proteins and in the presentation of antigens at the cell surface, thereby participating in the immune response (see Bitzer et al. 2016).

cell surface and presented by MHC class I molecules, enabling the immune system to tolerate self-antigens, while identifying and eliminating virally infected and cancerous cells that expose non-self-antigens (Anton and Yewdell 2014; Rock et al. 2014). According to the DRiP hypothesis, these antigenic peptides are predominantly generated from defective newly synthesized proteins (Anton and Yewdell 2014; Rock et al. 2014). DRiPs that serve as antigenic peptides may not be randomly generated but may derive from a selection of peptidogenic substrates, for example from proteins that are destined to a particular compartment. Third, the BAG6 gene is located on human chromosome 6, within the MHC class III region, and BAG6 expression is strongly upregulated upon treatment of antigen-presenting cells with inflammatory cytokine interferon γ (IFN-γ), which initiates the adaptive immune response (Kamper et al. 2012). Although the exact function of BAG6 in the context of antigen presentation is still under debate, recent evidence supports a role of BAG6 in promoting proteasome-mediated degradation of antigens (Bitzer et al. 2016), strengthening the link between BAG6, DRiPs, immunoproteasomes and antigen processing (Fig. 6). Fourth, a fraction of BAG6 associates with ribosomes that are synthesizing nascent membrane proteins to regulate the ubiquitination and proteasome-mediated degradation of membrane proteins that have been erroneously processed or exhibit non-inserted hydrophobic domains (Hessa et al. 2011). Fifth, together with VCP, BAG6 promotes the cytosolic degradation of newly synthesized ER substrates via two distinct processes, namely endoplasmic reticulum–associated degradation (ERAD) and ER stress–induced pre-emptive quality control (ER pQC) (Kadowaki et al. 2015; Wang et al. 2011) (Fig. 6). Together, these data support the notion that BAG6 targets a specific subset of DRiPs presumably to enhance the cellular immune response and clearly demonstrate that the subset of DRiPs handled by BAG6 is not targeted to SGs. Conversely, SGs are sensitive to the subset of DRiPs bound by HSPB8 and HSP70, whose processing is influenced by BAG3 (Ganassi et al. 2016; Mediani et al. 2019).

Considering that BAG6 is involved in the clearance of a relatively small pool of DRiPs (its depletion does not completely abrogate DRiP disposal; Fig. 1) and that, compared with BAG3 and BAG1, BAG6 possesses a non-canonical BAG domain that does not act as a bona fide BAG domain to cooperate with Hsc70/HSP70 (Mock et al. 2015), our data suggest that BAG3 and BAG6 bind to distinct pools of DRiPs, thereby exerting distinct functions. BAG3

ensures the compartmentalization and processing of HSP70-bound DRiPs, participating in the maintenance of proteostasis and granulostasis upon stress; in contrast, BAG6 binds directly to a subset of DRiPs, including ER-derived DRiPs and aberrant membrane proteins, proteasomes, and immunoproteasomes to facilitate their disposal, thus contributing to the maintenance of ER homeostasis and to the immune response (Fig. 6).

Accumulation of DRiPs and misfolded proteins in SGs, nucleoli, and PML nuclear bodies promotes their conversion into a non-dynamic dysfunctional state and is prevented by the HSP70 and VCP chaperones (Frottin et al. 2019; Ganassi et al. 2016; Mateju et al. 2017; Mediani et al. 2019; Turakhiya et al. 2018). Altered SG dynamics, nucleolar stress, and loss of proteostasis are important emerging pathomechanisms in ALS and other neurodegenerative diseases (Frottin et al. 2019; Lee et al. 2016; Mandrioli et al. 2019; White et al. 2019; Zhang et al. 2019). Thus, future lines of research should focus on the identification of the subsets of DRiPs that accumulate in specific cellular compartments and the specific types of chaperone machinery that are responsible for their clearance. This will enable us to identify which chaperones and co-chaperones should be pharmacologically targeted for therapeutic purposes.

Acknowledgments S.C. is grateful to CIGS (https://www.cigs.unimore.it/) for technical support with microscopy experiments and image analysis.

Funding information S.C. and S.A. were funded by the EU Joint Programme–Neurodegenerative Disease Research (JPND) (CureALS); S.C., J.M., C.C., and O.P. were funded by AriSLA (Granulopathy, MLOpathy, and RAPALS) and AIFA (co-ALS). S.C. was funded by MAECI (Dissolve ALS) and MIUR (Departments of excellence 2018-2022; E91I18001480001 and PRIN 2017 EX_ALS).

Compliance with ethical standards

Conflict of interest Simon Alberti is a scientific advisor of Dewpoint Therapeutics. All other authors declare no conflict of interest.

References

Alexander EJ et al (2018) Ubiquilin 2 modulates ALS/FTD-linked FUS-RNA complex dynamics and stress granule formation. Proc Natl Acad Sci U S A 115:E11485–E11494. https://doi.org/10.1073/pnas.1811997115

Anderson P, Kedersha N (2002a) Stressful initiations. J Cell Sci 115:3227–3234

Anderson P, Kedersha N (2002b) Visibly stressed: the role of eIF2, TIA-1, and stress granules in protein translation. Cell Stress Chaperones 7:213–221

Anton LC, Yewdell JW (2014) Translating DRiPs: MHC class I immunosurveillance of pathogens and tumors. J Leukoc Biol 95:551–562. https://doi.org/10.1189/jlb.1113599

Aulas A, Fay MM, Lyons SM, Achorn CA, Kedersha N, Anderson P, Ivanov P (2017) Stress-specific differences in assembly and composition of stress granules and related foci. J Cell Sci 130:927–937. https://doi.org/10.1242/jcs.199240

Balchin D, Hayer-Hartl M, Hartl FU (2016) In vivo aspects of protein folding and quality control. Science 353:aac4354. https://doi.org/10.1126/science.aac4354

Bitzer A, Basler M, Groettrup M (2016) Chaperone BAG6 is dispensable for MHC class I antigen processing and presentation. Mol Immunol 69:99–105. https://doi.org/10.1016/j.molimm.2015.11.004

Buchan JR, Kolaitis RM, Taylor JP, Parker R (2013) Eukaryotic stress granules are cleared by autophagy and Cdc48/VCP function. Cell 153:1461–1474

Carra S, Seguin SJ, Lambert H, Landry J (2008a) HspB8 chaperone activity toward poly(Q)-containing proteins depends on its association with Bag3, a stimulator of macroautophagy. J Biol Chem 283:1437–1444

Carra S, Seguin SJ, Landry J (2008b) HspB8 and Bag3: a new chaperone complex targeting misfolded proteins to macroautophagy. Autophagy 4:237–239

Chitiprolu M et al (2018) A complex of C9ORF72 and p62 uses arginine methylation to eliminate stress granules by autophagy. Nat Commun 9:2794. https://doi.org/10.1038/s41467-018-05273-7

Claessen JH, Ploegh HL (2011) BAT3 guides misfolded glycoproteins out of the endoplasmic reticulum. PloS one 6:e28542. https://doi.org/10.1371/journal.pone.0028542

Decker CJ, Parker R (2012) P-bodies and stress granules: possible roles in the control of translation and mRNA degradation. Cold Spring Harb Perspect Biol 4:a012286. https://doi.org/10.1101/cshperspect.a012286

Defenouillere Q et al (2013) Cdc48-associated complex bound to 60S particles is required for the clearance of aberrant translation products. Proc Natl Acad Sci U S A 110:5046–5051

Demand J, Alberti S, Patterson C, Hohfeld J (2001) Cooperation of a ubiquitin domain protein and an E3 ubiquitin ligase during chaperone/proteasome coupling. Curr Biol 11:1569–1577

Farny NG, Kedersha NL, Silver PA (2009) Metazoan stress granule assembly is mediated by P-eIF2alpha-dependent and -independent mechanisms. RNA 15:1814–1821. https://doi.org/10.1261/rna.1684009

Fecto F, Yan J, Vemula SP, Liu E, Yang Y, Chen W, Zheng JG, Shi Y, Siddique N, Arrat H, Donkervoort S, Ajroud-Driss S, Sufit RL, Heller SL, Deng HX, Siddique T (2011) SQSTM1 mutations in familial and sporadic amyotrophic lateral sclerosis. Arch Neurol 68:1440–1446

Frottin F et al (2019) The nucleolus functions as a phase-separated protein quality control compartment. Science. https://doi.org/10.1126/science.aaw9157

Frydman J (2001) Folding of newly translated proteins in vivo: the role of molecular chaperones. Annu Rev Biochem 70:603–647. https://doi.org/10.1146/annurev.biochem.70.1.603

Fuchs M, Poirier DJ, Seguin SJ, Lambert H, Carra S, Charette SJ, Landry J (2009) Identification of the key structural motifs involved in HspB8/HspB6-Bag3 interaction. The Biochemical journal 425:245–255

Gamerdinger M, Kaya AM, Wolfrum U, Clement AM, Behl C (2011) BAG3 mediates chaperone-based aggresome-targeting and selective autophagy of misfolded proteins. EMBO reports 12:149–156

Ganassi M et al (2016) A surveillance function of the HSPB8-BAG3-HSP70 chaperone complex ensures stress granule integrity and dynamism. Mol Cell 63:796–810. https://doi.org/10.1016/j.molcel.2016.07.021

Gentilella A, Khalili K (2011) BAG3 expression in glioblastoma cells promotes accumulation of ubiquitinated clients in an Hsp70-dependent manner. J Biol Chem 286:9205–9215. https://doi.org/10.1074/jbc.M110.175836

Grousl T, Ivanov P, Frydlova I, Vasicova P, Janda F, Vojtova J, Malinska K, Malcova I, Novakova L, Janoskova D, Valasek L, Hasek J (2009) Robust heat shock induces eIF2alpha-phosphorylation-independent assembly of stress granules containing eIF3 and 40S ribosomal subunits in budding yeast, *Saccharomyces cerevisiae*. J Cell Sci 122: 2078–2088. https://doi.org/10.1242/jcs.045104

Guilbert SM, Lambert H, Rodrigue MA, Fuchs M, Landry J, Lavoie JN (2018) HSPB8 and BAG3 cooperate to promote spatial sequestration of ubiquitinated proteins and coordinate the cellular adaptive response to proteasome insufficiency. FASEB J 32:3518–3535. https://doi.org/10.1096/fj.201700558RR

Hageman J, Kampinga HH (2009) Computational analysis of the human HSPH/HSPA/DNAJ family and cloning of a human HSPH/HSPA/DNAJ expression library. Cell Stress Chaperones 14:1–21. https://doi.org/10.1007/s12192-008-0060-2

Hartl FU, Hayer-Hartl M (2002) Molecular chaperones in the cytosol: from nascent chain to folded protein. Science 295:1852–1858. https://doi.org/10.1126/science.1068408

Hessa T, Sharma A, Mariappan M, Eshleman HD, Gutierrez E, Hegde RS (2011) Protein targeting and degradation are coupled for elimination of mislocalized proteins. Nature 475:394–397. https://doi.org/10.1038/nature10181

Ivanov P, Kedersha N, Anderson P (2019) Stress granules and processing bodies in translational control. Cold Spring harb Perspect Biol:11. https://doi.org/10.1101/cshperspect.a032813

Johnson JO, Mandrioli J, Benatar M, Abramzon Y, van Deerlin V, Trojanowski JQ, Gibbs JR, Brunetti M, Gronka S, Wuu J, Ding J, McCluskey L, Martinez-Lage M, Falcone D, Hernandez DG, Arepalli S, Chong S, Schymick JC, Rothstein J, Landi F, Wang YD, Calvo A, Mora G, Sabatelli M, Monsurrò MR, Battistini S, Salvi F, Spataro R, Sola P, Borghero G, ITALSGEN Consortium, Galassi G, Scholz SW, Taylor JP, Restagno G, Chiò A, Traynor BJ (2010) Exome sequencing reveals VCP mutations as a cause of familial ALS. Neuron 68:857–864

Kadowaki H et al (2015) Pre-emptive quality control protects the ER from protein overload via the proximity of ERAD components and SRP. Cell reports 13:944–956. https://doi.org/10.1016/j.celrep.2015.09.047

Kamper N, Franken S, Temme S, Koch S, Bieber T, Koch N (2012) gamma-Interferon-regulated chaperone governs human lymphocyte antigen class II expression. FASEB J 26:104–116. https://doi.org/10.1096/fj.11-189670

Kawahara H, Minami R, Yokota N (2013) BAG6/BAT3: emerging roles in quality control for nascent polypeptides. J Biochem 153:147–160. https://doi.org/10.1093/jb/mvs149

Kedersha N, Anderson P (2002) Stress granules: sites of mRNA triage that regulate mRNA stability and translatability. Biochem Soc Trans 30:963–969

Kedersha N, Ivanov P, Anderson P (2013) Stress granules and cell signaling: more than just a passing phase? Trends Biochem Sci 38: 494–506. https://doi.org/10.1016/j.tibs.2013.07.004

Knutsen JH, Rodland GE, Boe CA, Haland TW, Sunnerhagen P, Grallert B, Boye E (2015) Stress-induced inhibition of translation independently of eIF2alpha phosphorylation. J Cell Sci 128:4420–4427. https://doi.org/10.1242/jcs.176545

Kwon I et al (2014) Poly-dipeptides encoded by the C9orf72 repeats bind nucleoli, impede RNA biogenesis, and kill cells. Science 345:1139–1145. https://doi.org/10.1126/science.1254917

Lee KH et al (2016) C9orf72 dipeptide repeats impair the assembly, dynamics, and function of membrane-less organelles. Cell 167: 774-788 e717. https://doi.org/10.1016/j.cell.2016.10.002

Leznicki P, Clancy A, Schwappach B, High S (2010) Bat3 promotes the membrane integration of tail-anchored proteins. J Cell Sci 123: 2170–2178. https://doi.org/10.1242/jcs.066738

Mandrioli J, Mediani L, Alberti S, Carra S (2019) ALS and FTD: where RNA metabolism meets protein quality control. Semin Cell Dev Biol. https://doi.org/10.1016/j.semcdb.2019.06.003

Marrone L et al (2018) Isogenic FUS-eGFP iPSC reporter lines enable quantification of FUS stress granule pathology that is rescued by drugs inducing autophagy. Stem cell reports 10:375–389. https://doi.org/10.1016/j.stemcr.2017.12.018

Mateju D et al (2017) An aberrant phase transition of stress granules triggered by misfolded protein and prevented by chaperone function. EMBO J 36:1669–1687. https://doi.org/10.15252/embj.201695957

Mazroui R, Di Marco S, Kaufman RJ, Gallouzi IE (2007) Inhibition of the ubiquitin-proteasome system induces stress granule formation. Mol Biol Cell 18:2603–2618

Mediani L et al (2019) Defective ribosomal products challenge nuclear function by impairing nuclear condensate dynamics and immobilizing ubiquitin. EMBO J:e101341. https://doi.org/10.15252/embj.2018101341

Meriin AB, Narayanan A, Meng L, Alexandrov I, Varelas X, Cisse SMY II (2018) Hsp70-Bag3 complex is a hub for proteotoxicity-induced signaling that controls protein aggregation. Proc Natl Acad Sci U S A. https://doi.org/10.1073/pnas.1803130115

Minami R, Hayakawa A, Kagawa H, Yanagi Y, Yokosawa H, Kawahara H (2010) BAG-6 is essential for selective elimination of defective proteasomal substrates. J Cell Biol 190:637–650. https://doi.org/10.1083/jcb.200908092

Minoia M, Boncoraglio A, Vinet J, Morelli FF, Brunsting JF, Poletti A, Krom S, Reits E, Kampinga HH, Carra S (2014) BAG3 induces the sequestration of proteasomal clients into cytoplasmic puncta: implications for a proteasome-to-autophagy switch. Autophagy 10:1603–1621

Mock JY, Chartron JW, Zaslaver M, Xu Y, Ye Y, Clemons WM Jr (2015) Bag6 complex contains a minimal tail-anchor-targeting module and a mock BAG domain. Proc Natl Acad Sci U S A 112:106–111. https://doi.org/10.1073/pnas.1402745112

Mock JY, Xu Y, Ye Y, Clemons WM Jr (2017) Structural basis for regulation of the nucleo-cytoplasmic distribution of Bag6 by TRC35. Proc Natl Acad Sci U S A 114:11679–11684. https://doi.org/10.1073/pnas.1702940114

Molliex A et al (2015) Phase separation by low complexity domains promotes stress granule assembly and drives pathological fibrillization. Cell 163:123–133

Murakami T et al (2015) ALS/FTD mutation-induced phase transition of FUS liquid droplets and reversible hydrogels into irreversible hydrogels impairs RNP granule function. Neuron 88:678–690

Murata S, Takahama Y, Tanaka K (2008) Thymoproteasome: probable role in generating positively selecting peptides. Curr Opin Immunol 20:192–196. https://doi.org/10.1016/j.coi.2008.03.002

Nedelsky NB, Taylor JP (2019) Bridging biophysics and neurology: aberrant phase transitions in neurodegenerative disease. Nat Rev Neurol. https://doi.org/10.1038/s41582-019-0157-5

Patel A, Lee HO, Jawerth L, Maharana S, Jahnel M, Hein MY, Stoynov S, Mahamid J, Saha S, Franzmann TM, Pozniakovski A, Poser I, Maghelli N, Royer LA, Weigert M, Myers EW, Grill S, Drechsel D, Hyman AA, Alberti S (2015) A liquid-to-solid phase transition of the ALS protein FUS accelerated by disease mutation. Cell 162: 1066–1077

Protter DSW, Parker R (2016) Principles and properties of stress granules trends. Cell Biol 26:668–679. https://doi.org/10.1016/j.tcb.2016.05.004

Qamar S et al (2018) FUS phase separation is modulated by a molecular chaperone and methylation of arginine Cation-pi interactions. Cell 173:720-734 e715. https://doi.org/10.1016/j.cell.2018.03.056

Qian SB, Princiotta MF, Bennink JR, Yewdell JW (2006) Characterization of rapidly degraded polypeptides in mammalian

cells reveals a novel layer of nascent protein quality control. J Biol Chem 281:392–400. https://doi.org/10.1074/jbc.M509126200

Rauch JN, Gestwicki JE (2014) Binding of human nucleotide exchange factors to heat shock protein 70 (Hsp70) generates functionally distinct complexes in vitro. J Biol Chem 289:1402–1414. https://doi.org/10.1074/jbc.M113.521997

Rock KL, Farfan-Arribas DJ, Colbert JD, Goldberg AL (2014) Re-examining class-I presentation and the DRiP hypothesis. Trends Immunol 35:144–152. https://doi.org/10.1016/j.it.2014.01.002

Schubert U, Anton LC, Gibbs J, Norbury CC, Yewdell JW, Bennink JR (2000) Rapid degradation of a large fraction of newly synthesized proteins by proteasomes. Nature 404:770–774

Seguin SJ, Morelli FF, Vinet J, Amore D, de Biasi S, Poletti A, Rubinsztein DC, Carra S (2014) Inhibition of autophagy, lysosome and VCP function impairs stress granule assembly. Cell Death Differ 21:1838–1851

Sidrauski C, McGeachy AM, Ingolia NT, Walter P (2015) The small molecule ISRIB reverses the effects of eIF2alpha phosphorylation on translation and stress granule assembly. eLife 4. https://doi.org/10.7554/eLife.05033

Szeto J et al (2006) ALIS are stress-induced protein storage compartments for substrates of the proteasome and autophagy. Autophagy 2:189–199. https://doi.org/10.4161/auto.2731

Takayama S, Reed JC (2001) Molecular chaperone targeting and regulation by BAG family proteins. Nat Cell Biol 3:E237–E241

Taylor JP, Brown RH Jr, Cleveland DW (2016) Decoding ALS: from genes to mechanism. Nature 539:197–206. https://doi.org/10.1038/nature20413

Thedieck K et al (2013) Inhibition of mTORC1 by astrin and stress granules prevents apoptosis in cancer cells. Cell 154:859–874. https://doi.org/10.1016/j.cell.2013.07.031

Tourriere H, Chebli K, Zekri L, Courselaud B, Blanchard JM, Bertrand E, Tazi J (2003) The RasGAP-associated endoribonuclease G3BP assembles stress granules. J Cell Biol 160:823–831. https://doi.org/10.1083/jcb.200212128

Turakhiya A et al (2018) ZFAND1 recruits p97 and the 26S proteasome to promote the clearance of arsenite-induced stress granules. Mol Cell 70:906-919 e907. https://doi.org/10.1016/j.molcel.2018.04.021

Verma R, Oania RS, Kolawa NJ, Deshaies RJ (2013) Cdc48/p97 promotes degradation of aberrant nascent polypeptides bound to the ribosome. eLife 2:e00308

Wang HQ, Liu HM, Zhang HY, Guan Y, Du ZX (2008) Transcriptional upregulation of BAG3 upon proteasome inhibition. Biochem Biophys Res Commun 365:381–385. https://doi.org/10.1016/j.bbrc.2007.11.001

Wang Q, Liu Y, Soetandyo N, Baek K, Hegde R, Ye Y (2011) A ubiquitin ligase-associated chaperone holdase maintains polypeptides in soluble states for proteasome degradation. Mol Cell 42:758–770. https://doi.org/10.1016/j.molcel.2011.05.010

White MR et al (2019) C9orf72 poly(PR) dipeptide repeats disturb biomolecular phase separation and disrupt Nucleolar function. Mol Cell 74:713-728 e716. https://doi.org/10.1016/j.molcel.2019.03.019

Zhang P, Fan B, Yang P, Temirov J, Messing J, Kim HJ, Taylor JP (2019) Chronic optogenetic induction of stress granules is cytotoxic and reveals the evolution of ALS-FTD pathology. eLife:8. https://doi.org/10.7554/eLife.39578